

REMOVAL OF FLUORIDE FROM AQUEOUS SOLUTION BY NICKEL OXIDE NANOPARTICLES: EQUILIBRIUM AND KINETIC STUDIES

Chinenye Adaobi Igwegbe,^a Somayeh Rahdar,^b Abbas Rahdar,^c Amir Hossein Mahvi,^d Shahin Ahmadi,^{b,*} Artur Marek Banach^e

Awka, Nigeria; Zabol and Tehran, Iran; and Lublin, Poland

ABSTRACT: Fluoride (F) in high concentration is very hazardous to human health. The efficacy of nickel oxide nanoparticles (NiO NPs) was investigated in this research as an adsorbent for the elimination of fluoride from aqueous solutions. The effects of pH, contact time, initial concentration of F, and adsorbent dosage on the performance of NiO NPs in the removal of fluoride from aqueous solutions were investigated at room temperature. Langmuir, Freundlich, Temkin, Koble-Corrigan, and Redlich-Peterson adsorption isotherms were employed for the analysis of the adsorption process. Maximum adsorption was achieved at 60 min at pH 5, an adsorbent dosage of 0.02 g/L, and an initial fluoride concentration of 20 mg/L. The results also showed that fluoride adsorption by NiO NPs was more compatible with the Freundlich isotherm ($R^2 = 0.999$), and that the process followed the pseudo-second-order kinetic, Ho (type I) ($R^2 = 0.9999$ and $R^2 = 0.9997$ at 20 and 25 mg/L fluoride concentrations, respectively). From the results obtained, it can be concluded that NiO NPs can be used with high efficiency for fluoride removal.

Keywords: Aqueous solution; Fluoride; Isotherm; Kinetic; Nickel oxide nanoparticles.

INTRODUCTION

The fluoride ion (F^-) is one of the soluble ions in aqueous sources.¹ Fluoride compounds are found in industrial applications and they are applied widely in the production of semiconductors, fertilizers, high purity graphite, and aluminum.²⁻³ A high concentration of fluoride can lead to dental, skeletal, and non-skeletal fluorosis. Fluorosis weakens the skeletal and dental structures and in extreme cases it can result in paralysis and death.⁴ More than 30 million people have been affected by fluorosis and 100 million people have been exposed to the risk of developing fluorosis.⁵ The long term effects of fluoride exposure and its accumulation not only result in skeletal and dental risks but may also change the DNA structure and optimal power.⁵⁻⁶ The upper level of fluoride in drinking water recommended by the World Health Organization (WHO) is 1.5 mg/L.⁷ A high concentration of fluoride is toxic and may result in non-skeletal fluorosis with digestive disorders, liver impairment, and endocrine damage including thyroid hormone disturbances and a decrease in growth hormone.⁸ Fluoride has a great influence on the metabolism of some elements such as calcium and potassium.⁹ Fluoride contamination is a worldwide problem especially in Africa, Asia, and the USA.¹⁰ Fluoride must be properly treated before being discharged to water bodies.⁷ Various methods, such as adsorption by activated alumina, ion exchange, reverse osmosis, electro dialysis, adsorption, electrocoagulation, and chemical treatment, have been used for fluoride reduction but most of them have some disadvantages such as high maintenance and operation

^aDepartment of Chemical Engineering, Nnamdi Azikiwe University, Awka, Nigeria; ^bDepartment of Environmental Health, Zabol University of Medical Sciences, Zabol, Iran; ^cFaculty of Science, University of Zabol, Zabol, Iran; ^dCenter for Solid Waste Research, Institute for Environmental Research, Tehran University of Medical Sciences, Tehran, Iran; ^eDepartment of Biochemistry and Environmental Chemistry, Institute of Biotechnology, The John Paul II Catholic University of Lublin, Konstantynów 11 Str, 20708 Lublin, Poland, Tel. +4881 454 54 42; E-mail: abanach@kul.pl; For correspondence: Shahin Ahmadi, Department of Environmental Health, Zabol University of Medical Sciences, Zabol, Iran; E-mail: sh.ahmadi398@gmail.com

costs, secondary contamination, and complexity of the refining method.¹¹⁻¹⁶ Physical adsorption is an effective and affordable method. The adsorption of fluoride by different adsorbents such as activated carbon have been studied.¹⁷ Recently, some of the features of metal oxide nanoparticles, such as high surface area and unusual adsorptive properties, have led to an interest in nanoparticle synthesis and use.¹⁸ The structural quality of elements would be better in nano dimensions.¹⁹ Nickel oxide nanoparticles (NiO NPs) are a significant metallic oxide because of their magnetic and chemical properties. The chemical and physical properties of nanoparticles are related to the techniques used for their synthesis.²⁰ Nanoparticles can be used as a catalyst in the oxidation of inorganic compounds.²⁰⁻²¹ Ultrafine NiO particles of the same size are used widely in different fields such as in the production of films, magnetic elements, ceramics, and batteries.²¹

The main purpose of this study is to investigate the efficiency of NiO NPs in the adsorption of fluoride from an aqueous solution. The adsorption process was also studied by applying adsorption isotherm and kinetic models.

MATERIALS AND METHODS

Synthesis of nickel oxide nanoparticles (NiO NPs): The NiO NPs were prepared by using NiCl₂·6H₂O and NaOH as the starting materials and double-distilled water as the dispersing solvent. The NiO NPs were prepared by the co-precipitation method using previously described methods.²² At first, 5.9412 g of NiCl₂·6H₂O was dissolved in 250 mL of double-distilled water as solvent to get a certain molar concentration at room temperature. Then, the obtained solution was stirred magnetically at 50°C for 40 min. Ten mL of NaOH with a certain molarity was then added dropwise to the solution until the pH reached pH 8. The nanoparticles of NiO were synthesized using the chemical reaction:



The obtained green gel was washed with distilled water and then ethanol to remove any byproducts formed during the reaction process and dried at 60°C for 14 hr. The dried samples were calcined (annealed) at 300°C for 2 hr to obtain NiO NPs. The color of the sample changed from green to black because of the annealing process.

The properties of the studied nanomaterial were determined using a series of analytical methods. Fourier-transform infrared spectroscopy (FT-IR) was done on a JASCO 640 plus machine (4000-400 cm⁻¹) at room temperature; X-ray powder diffraction (XRD) was carried out on a D8 Advance X'Pert X-Ray diffractometer (Bruker); field emission scanning electron microscopy (FESEM) was carried out using a Mira 3-XMU instrument; and vibrating magnetometry (VSM) was analyzed using a Kavir Precise Magnetic instrument (MDKFT, Iran).

Adsorption experiments: All the reagents used were of at least of analytical grade and purchased from Merck, Germany. All the solutions were prepared using de-ionized water. The adsorbent was added to each 1 L of water sample containing various concentrations of fluoride (F). The pH of the water sample was adjusted by adding 0.1 N HCl or 0.1 N NaOH. The adsorption process were studied by

considering the effects of different parameters, such as pH (3, 5, 6, 7, and 9), contact time (20, 30, 45, 60, and 100 min), initial F concentration (5, 10, 20, and 25 mg/L) and NiO NPs dosage (0.02, 0.05, 0.06, 0.07, and 0.09 g/L). To create the optimal conditions, a shaker with 150 rpm was used. The initial and final F concentrations in the solution were analyzed by a UV–visible recording spectrophotometer (Shimadzu Model: CE-1021-UK construction, Japan) and was determined at a maximum absorbance (λ_{\max}) of 570 nm,²³ which is the characteristic wavelength of F. The pH was measured using a MIT65 pH meter. The removal efficiency, %R, and the amount of F adsorbed, q_e (mg/g) were calculated based on the following formulas:^{24, 25}

$$\%R = \frac{(C_0 - C_f)}{C_0} \times 100 \quad (1)$$

$$q_e = (C_0 - C_e) \times \frac{V}{M} \quad (2)$$

Where, C_0 and C_f are the initial and residual F concentrations, respectively. M is the weight of NiO NPs (g) and V is the volume of the solution (L). C_e is the final equilibrium liquid phase concentration of F (mg/g).

RESULTS AND DISCUSSION

Characterization of the synthetic nano NiO: Figure 1 shows the SEM image of the NiO NPs. The working instrumental parameters of 5.997 mm working distance,

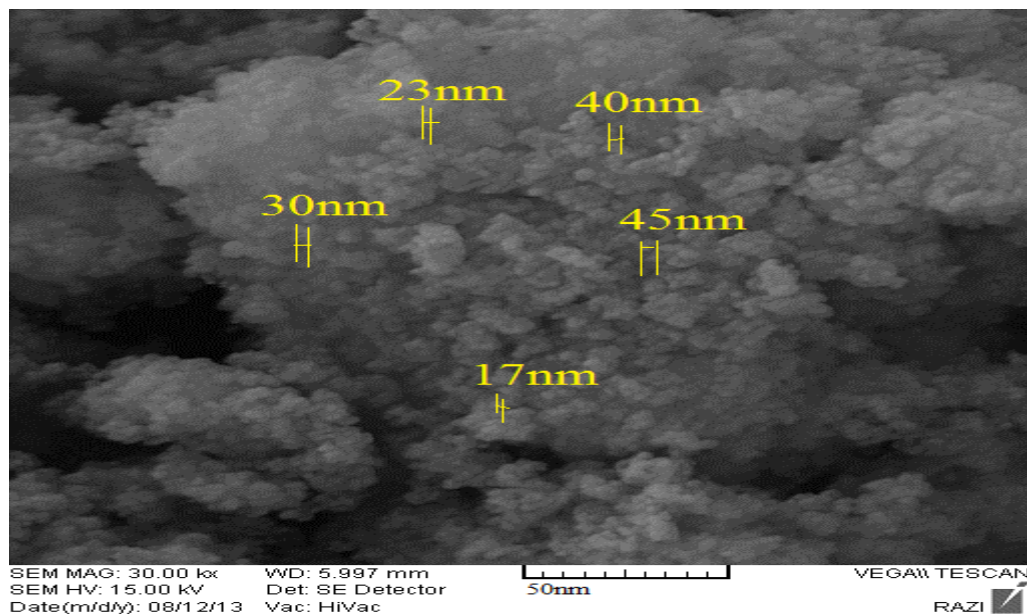


Figure 1. SEM image of NiO NPs.

The figure seems to be rough with sponge-like clusters and is also spherical in shape. A high level of porosity was observed on the synthesized NiO NPs. Different particle sizes of 17, 23, 30, 40, and 45 nm, with an average particle size of 31 nm, were observed on the sample due to the fact that the NiO NPs can agglomerate due to its high surface kinetic energy. The SEM image also indicates that the units used are nanometers which implies that the NiO NPs are nanoparticles

The FTIR spectra of a nanoparticle of NiO is shown in Figure 2 (plot of IR transmittance against wave number).

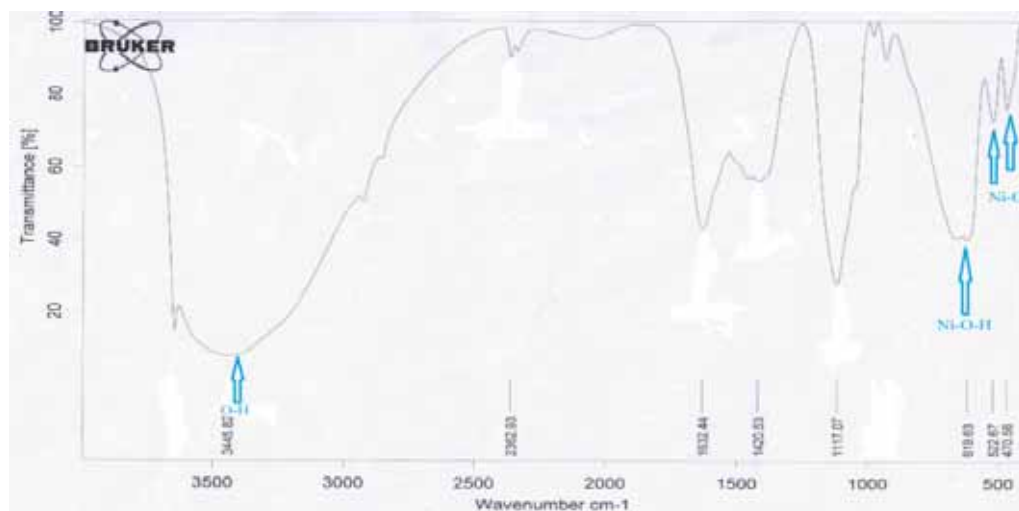


Figure 2. FT-IR of NiO NPs

The FTIR analysis of NiO NPs indicates the presence of sharp and strong C – H stretch bend of alkynes (619.63 cm^{-1}), the C – N stretch of aliphatic amines (1117.07 cm^{-1}), and the C – C stretch of aromatics (1420.53 cm^{-1}), the N–H bend of $1\times$ amines (1632.44 cm^{-1}), and the C = N stretch of nitriles (2362.93 cm^{-1}) and the H–bonded O – H stretch of alcohols (3445.82 cm^{-1}). The O – H stretch in alcohols, which is a very strong and broad bond, was detected in the NiO NPs and they are important sites for adsorption.²⁶ The effect of the hydroxyl group (O – H) is experienced more because the hydrogen bonding with other hydroxyl bonds does not exist in isolation and forms a stable structure^{27, 28}.

The value-stream mapping (VSM) is a lean-management method for analyzing the current state and designing a future state for the series of events that take a product or service from its beginning through to the customer. Magnetization measurements of NiO NPs were performed using VSM technique at fields of -8000 to 8000 emu/g (before and after calcinations, respectively) and stored at room temperature which are shown in Figure 3. It was observed that the NiO NPs with the smallest particle size produced a higher value of saturation magnetization (0.8 emu/g).

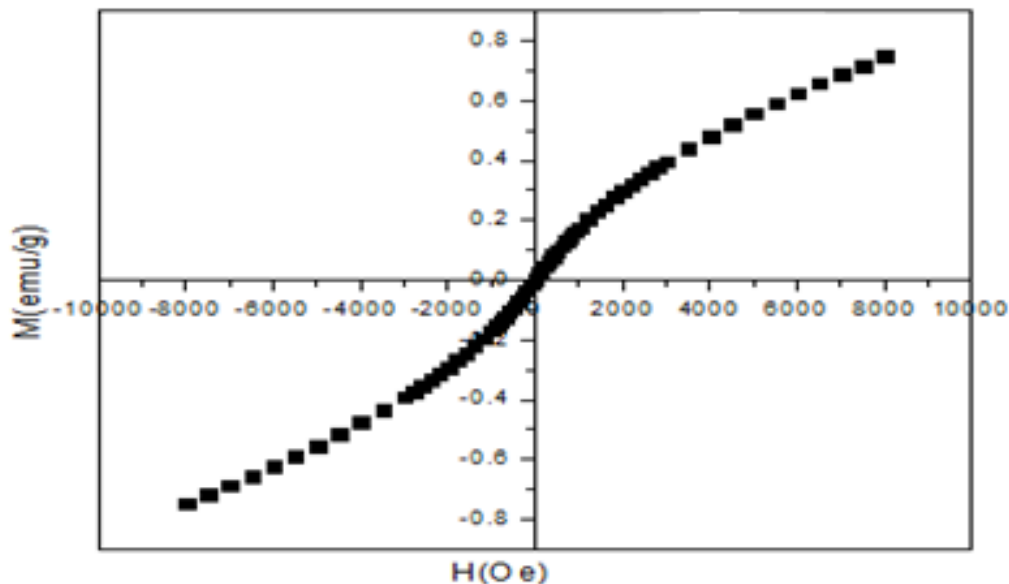


Figure 3. VSM hysteresis loop of magnetic nano-adsorbent

Effect of initial pH and adsorbent dose: The effect of differences in pH (3 – 9) on the adsorption of fluoride (F) onto the NiO NPs with a contact time of 30 min, an initial fluoride concentration of 20 mg/L, and an adsorbent dosage of 0.09 mg/L are shown in Figure 4.

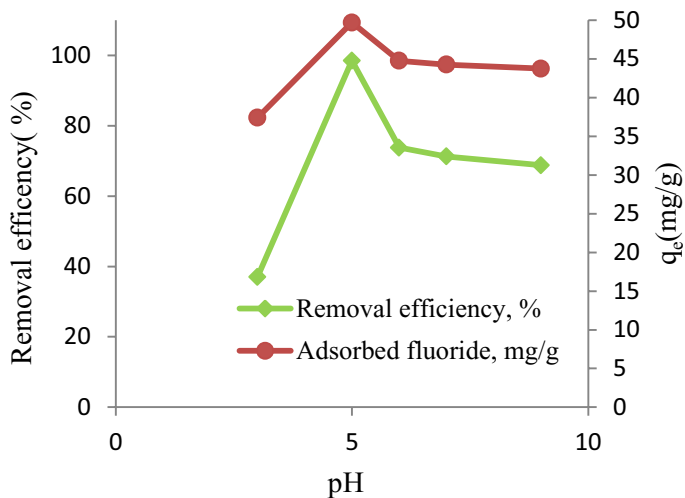


Figure 4. Effect of pH on F adsorption onto NiO NPs. (Time: 30 min, dosage: 0.09 mg/L, initial F concentration: 10 mg/L).

When the pH was increased from pH 3 to pH 5, the removal percentage increased from 36.99 to 98.5 %, respectively. The removal percentage decreased

when the pH was increased from pH 6 to pH 9. The amount of fluoride adsorbed also increased from 37.39 mg/g to 49.7 mg/g when the pH was increased from pH 3 to pH 5. An increased amount of H^+ , a reduction of OH^- , and an increase of positive ions reduce the efficiency of the absorbent surface.²⁹ F in aqueous solution has a negative charge and this results in an increase in the adsorption efficiency at low pH. At a low pH, the adsorbent surface possesses a positive charge.^{29, 30}

The effect of the adsorbent dose on the removal of F was studied by varying the dose of adsorbent from 0.02 to 0.09 g/L. From Figure 5, it is evident that the adsorbent dose significantly influenced the amount of F adsorbed.

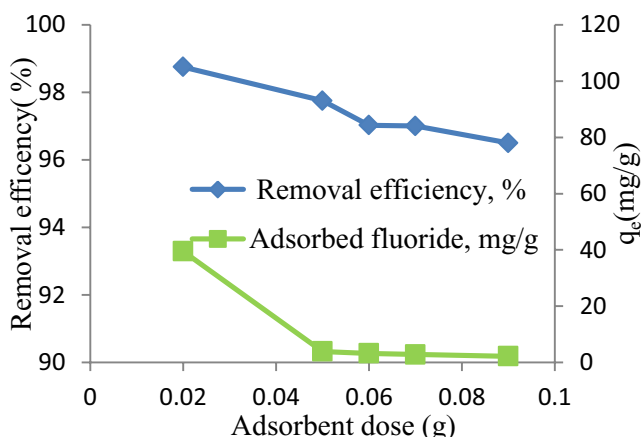


Figure 5. Effect of adsorbent dosage on F adsorption onto NiO NPs. (Time: 30 min, pH: 5, initial F concentration: 10 mg/L)

When the adsorbent concentration was increased from 0.02 to 0.09 g/L at an initial F concentration 10 mg/L, the efficiency decreased from 98.75% to 96.5%. The biosorption capacity (q_e) of the NiO NPs also decreased from 39.5 to 2.2 mg/g when the NiO NPs dosage was increased from 0.02 to 0.09 g/L. In fact, the level of deletion significantly depends on the number of active sites and by increasing the dosage of nanoparticles to an appropriate level, the number of available adsorption sites will decrease as a result of a decreased adsorption capacity.³⁰

Effect of contact time and initial F concentration: Figure 6 shows the adsorption efficiency versus time at different F concentrations. The time of equilibrium was very short. The maximum removal efficiency of the different fluoride concentrations was observed at the contact time of 60 min. The removal efficiency was higher at the earlier times. After this time, the slope of diagram slowed and at a specific time reached equilibrium. The F adsorption in the initial minutes was high but, after a while, the absorption rate decreased because of a reduced fluoride concentration and a reduction of the active sites present in adsorbent surface.³¹ The active sites were available in the initial steps and after starting the reaction, they were all occupied with F molecules. The adsorption rate was decreased at the initial F concentrations of 20 and 25 mg/L because of a decrease in the active sites.³²

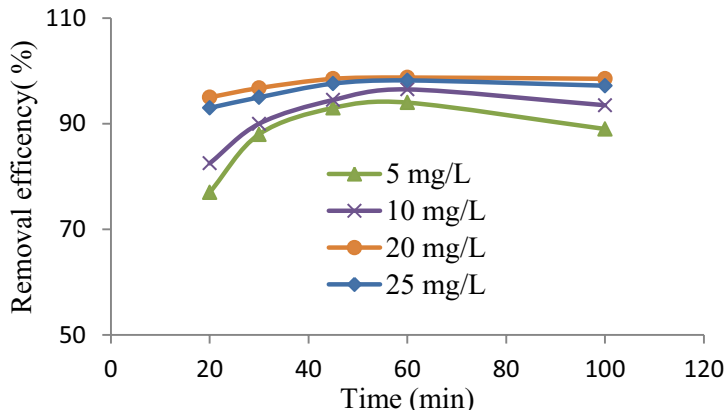


Figure 6. Effect of time on F adsorption onto NiO NPs. (Dosage: 0.02 g/L, pH: 5)

Adsorption isotherms: Specifying the adsorption isotherms, the adsorption capacity, and the potential of the adsorption materials used for removing contaminants are considered to be some of the most important traits of the adsorbing material. The experiments to determine the adsorption isotherms were performed with an adsorbent amount of 0.02 g/L and a fluoride concentration of 20 mg/L at pH 5. The important parameter in designing the adsorption system is the prediction of the adsorption capacity. This can be obtained by analyzing the isotherm data. The adsorption isotherms equations used in the study are presented in Table 1.

Table 1. The isotherm equations used in the study^{33, 34, 35}

Isotherm model	Linear expression	Plot
Freundlich	$Log q_e = \frac{1}{n} \log C_e + \log k_f$	In q_e vs In C_e
	Type (I): $\frac{C_e}{q_e} = \frac{1}{q_m} \cdot \frac{1}{k_1} + \frac{C_e}{q_m}$	(C_e/q_e) vs C_e
	Type (II): $\frac{1}{q_e} = \frac{1}{q_m} + (\frac{1}{q_m K_L}) \frac{1}{C_e}$	$1/q_e$ vs $1/C_e$
Langmuir	Type (III): $q_e = q_m - (\frac{1}{K_L}) \frac{q_e}{C_e}$	q_e vs q_e/C_e
	Type (IV): $\frac{q_e}{c_e} = K_L q_m - K_L q_e$	q_e/C_e vs q_e
	Temkin	$q_e = q_m \ln K_T + q_m \ln C_e$
Koble-Corrigan	$(1/q_e) = (1/A_{KC} C_e^p) + (B_{KC}/A_{KC})$	$(1/q_e)$ vs $(1/C_e^p)$
Redlich-Peterson	$Ln[(A_{RP} C_e / q_e) - 1] = g \ln C_e + \ln B_{RP}$	$Ln[(A_{RP} C_e / q_e) - 1]$ vs In C_e

According to the obtained results (Table 2 and Figure 7), the experimental data is more compatible with the Freundlich isotherm. The basis for choosing the appropriate isotherm is the correlation coefficient, R^2 . The Freundlich adsorption isotherm gave an R^2 value of 0.999, which is higher than the R^2 value of the other adsorption isotherms. Moreover, if the variable $1/n$ is between 0 and 1, it indicates the heterogeneity of the process and that the adsorption will be desirable.³⁶

Table 2. Isotherms parameters obtained by linear regression method for the sorption of fluoride by NiO NPs

Isotherms		R^2	parameters
Freundlich		0.999	$K_F = 0.41 (\text{mg g}^{-1})(\text{L mg}^{-1})^{1/n}$; $1/n = 1.057$
Langmuir	Type(I)	0.886	$q_m = 1.63(\text{mg g}^{-1})$; $K_L = 2(\text{L mg}^{-1})$
	Type(II)	0.5093	$q_m = 1.16 (\text{mg g}^{-1})$; $K_L = 0.14(\text{L mg}^{-1})$
	Type(III)	0.7297	$q_m = 1.9(\text{mg g}^{-1})$; $K_L = 2.08(\text{L mg}^{-1})$
	Type(IV)	0.7062	$q_m = 1.1(\text{mg g}^{-1})$; $K_L = 2.6(\text{L mg}^{-1})$
Temkin		0.627	$q_m = 7.63(\text{mg g}^{-1})$; $K_T = 3.4(\text{L mg}^{-1})$
Koble-Corrigan		0.9311	$A_{KC} = 1.95(\text{mg g}^{-1})(\text{L mg}^{-1})^P$; $B_{KC} = 1.81(\text{L mg}^{-1})^P$; $P = 0.8$
Redlich-Peterson		0.673	$g = 0.08$; $B_{RP} = 1(\text{L mg}^{-1})g$; $A_{RP} = 2.9(\text{mg g}^{-1})(\text{L mg}^{-1})$

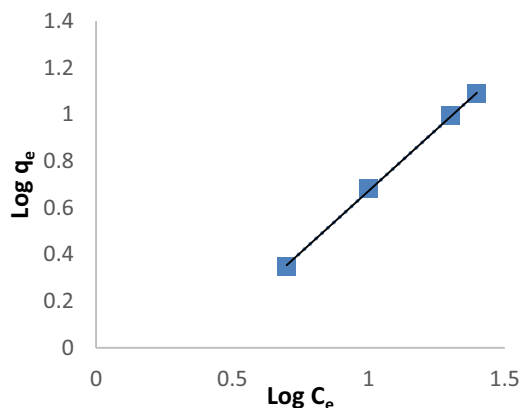


Figure 7. Freundlich isotherm plot of fluoride adsorption on NiO NPs.

Adsorption kinetics study: Adsorption kinetics was defined as the mechanism of adsorption with time. The models of Ho (Pseudo-second-order) and Lagergren (Pseudo-first-order) were applied to fit the adsorption kinetics. The kinetic model equations are shown in Table 3. The comparison and assessment of the correlation coefficient (R^2) shows the best kinetic model in accordance with the adsorption process. Table 4 shows the different values of the correlation coefficient achieved for the four kinetic models. The pseudo-second-order kinetic (Ho, Type (I)) showed the best correlation coefficient ($R^2 = 0.9999$ at $C_0 = 20 \text{ mg/L}$) (Table 4 and Figure 8).

Table 3. Kinetics parameters obtained by linear regression method for the sorption of fluoride by activated NiO NPs.³⁷

		Kinetic equations	
Lagergren		$Log(q_e - q_t) = \log q_e - \frac{k_1}{2.303}t$	
Ho	Type(I)	$\frac{t}{q_t} = \frac{1}{k_2 q_e^2} + \frac{t}{q_e}$	
	Type(II)	$\frac{t}{q_t} = \left(\frac{1}{k_2 q_e^2}\right)\frac{1}{t} + \frac{1}{q_e}$	
	Type(III)	$q_t = q_e - \left(\frac{1}{k q_e}\right)\frac{q_t}{t}$	

Table 4. The linear adsorption kinetic model constants for the removal of F

C ₀ (mg/l)	Lagergren				Ho (I)			Ho (II)			Ho (III)		
	q _{e,exp}	K ₁	q _e	R ²	K ₂	q _e	R ²	K ₂	q _e	R ²	K ₂	q _e	R ²
20	9.85	0.017	4.29	0.4727	0.007	12.3	0.9999	0.66	1.24	0.614	0.047	12.45	0.849
25	12.15	0.012	2.7	0.4244	0.006	12.3	0.9997	0.47	0.12	0.445	0.05	12.46	0.844

6

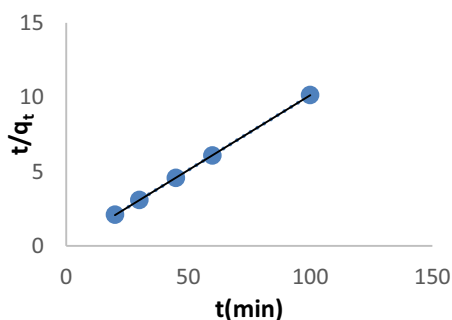


Figure 8. Pseudo-second-order, Ho (I) plot of fluoride adsorption on NiO NPs

Figure 8. Pseudo-second-order, Ho (I) plot of fluoride adsorption on NiO NPs.

CONCLUSIONS

In this research, we investigated the efficacy of nickel oxide nanoparticles (NiO NPs) as an adsorbent for the elimination of fluoride (F) from its aqueous solutions, including the effects of the pH, contact time, initial fluoride concentration, and adsorbent dosage. Langmuir, Freundlich, Temkin, Koble-Corrigan, and Redlich-Peterson adsorption isotherms were applied to fit the adsorption experimental data. From the results, the adsorption efficiency was increased by increasing the pH from 3 to 5 but decreased from pH 6 to 9. The adsorption efficiency was increased as the

contact time was increased. It was also found that with an increasing amount of NiO NPs adsorbent, the removal efficiency decreased. Maximum F removal was achieved at 60 min at pH 5, adsorbent dosage of 0.02 g/L, and an initial F concentration of 20 mg/L. The results revealed that the experimental data fitted the pseudo-second-order, Ho (type I) kinetic ($R^2 = 0.9999$ and $R^2 = 0.9997$ at 20 and 25 mg/L F concentrations, respectively) and the Freundlich isotherm ($R^2 = 0.999$) models. Based on the data obtained in this study, it can be concluded that the adsorption of F by NiO NPs is an efficient and reliable method for F removal from liquid solutions.

ACKNOWLEDGEMENT

This work was supported by a research grant of the Environmental Health Laboratory of Zabol Province, Iran, (Grant No. IR.ZBMU. REC-1396-335).

REFERENCES

- 1 Boldaji MR, Mahvi AH, Dobaradaran S, Hosseini SS. Evaluating the effectiveness of a hybrid sorbent resin in removing fluoride from water. *International Journal of Environmental Science and Technology* 2009;6(4):629-32.
- 2 Rahmani A, Rahmani K, Dobaradaran S, Mahvi AH, Mohamadjani R, Rahmani H. Child dental caries in relation fluoride and some inorganic constituents in drinking water in Arsanjan, Iran. *Fluoride* 2010;43(3):179-86.
- 3 Dobaradaran S, Fazelinia F, Mahvi AH, Hosseini SS. Particulate airborne fluoride from an aluminum production plant in Arak, Iran. *Fluoride* 2009;42(3):228-32.
- 4 Nouri J, Mahvi AH, Babaei A, Ahmadvpour E. Regional pattern distribution of groundwater fluoride in the Shush aquifer of Khuzestan County, Iran. *Fluoride* 2006;39(4):321-5.
- 5 Mahramanlioglu M, Kizilcikli I, Bicer I. Adsorption of fluoride from aqueous solution by acid treated spent bleaching earth. *Journal of Fluorine Chemistry* 2002;115(1):41-7.
- 6 Gupta VK, Ali I, Saini VK. Defluoridation of wastewaters using waste carbon slurry. *Water Research* 2007;41(15):3307-16.
- 7 WHO. Guidelines for drinking water quality. 4th ed. Geneva: WHO; 2011. p.371.
- 8 Leyva-Ramos R, Jacobo-Azuara A, Diaz-Flores P, Guerrero-Coronado R, Mendoza-Barron J, Berber-Mendoza M. Adsorption of chromium (VI) from an aqueous solution on a surfactant-modified zeolite. *Colloids and Surfaces A: Physicochemical and Engineering Aspects* 2008;330(1):35-41.
- 9 Hu K, Dickson JM. Nanofiltration membrane performance on fluoride removal from water. *Journal of Membrane Science* 2006;279(1):529-38.
- 10 Karimzade S, Aghaei M, Mahvi AH. Investigation of intelligence quotient in 9–12-year-old children exposed to high- and low-drinking water fluoride in west Azerbaijan province, Iran. *Fluoride* 2014;47(1):9-14.
- 11 Ghorai S, Pant K. Equilibrium, kinetics and breakthrough studies for adsorption of fluoride on activated alumina. *Separation and Purification Technology* 2005;42(3):265-71.
- 12 Hu K, Dickson JM. Nanofiltration membrane performance on fluoride removal from water. *Journal of Membrane Science* 2006;279(1):529-38.
- 13 Ghosh D, Medhi C, Purkait M. Treatment of fluoride containing drinking water by electrocoagulation using monopolar and bipolar electrode connections. *Chemosphere* 2008; 73(9):1393-400.
- 14 Sehn P. Fluoride removal with extra low energy reverse osmosis membranes: three years of large scale field experience in Finland. *Desalination* 2008;223(1-3):73-84.
- 15 Viswanathan N, Meenakshi S. Role of metal ion incorporation in ion exchange resin on the selectivity of fluoride. *Journal of Hazardous Materials* 2009;162(2):920-30.
- 16 Dehghani MH, Faraji M, Mohammadi A, Kamani H. Optimization of fluoride adsorption onto natural and modified pumice using response surface methodology: Isotherm, kinetic and thermodynamic studies. *Korean Journal of Chemical Engineering* 2017;34(2):454-6.
- 17 Meenakshi S, Viswanathan N. Identification of selective ion-exchange resin for fluoride sorption. *J Colloid Interface Sci* 2007;308:438-50.

- 579 Research report
Fluoride 52(4):569-579
October 2019
- Removal of fluoride from aqueous solution by nickel oxide nanoparticles: equilibrium and kinetic studies
Igwegbe, Rahdar, Rahdar, Mahvi, Ahmadi, Banach
- 18 Song Z, Chen L, Hu J, Richards R. NiO (111) nanosheets as efficient and recyclable adsorbents for dye pollutants removal from wastewater. *Nanotechnology* 2009;20(27):275707.
 - 19 Ahmadi S, Banach A, Mostafapour F. K, Balarak D. Study survey of cupric oxide nanoparticles in removal efficiency of ciprofloxacin antibiotic from aqueous solution: adsorption isotherm study. *Desalination and Water Treatment* 2017;89:297-303.
 - 20 Lai TL, Wang WF, Shu YY, Liu YT, Wang CB. Evaluation of microwave-enhanced catalytic degradation of 4-chlorophenol over nickel oxides. *Journal of Molecular Catalysis A: Chemical* 2007;273(1-2):303-9.
 - 21 Wang HC, Chang SH, Hung PC, Hwang JF, Chang MB. Catalytic oxidation of gaseous PCDD/Fs with ozone over iron oxide catalysts. *Chemosphere* 2008;71(2):388-97.
 - 22 Rahdar A, Aliahmad M, Azizi Y. NiO nanoparticles: synthesis and characterization. *Journal of Nanostructures* 2015;5(2):145-51.
 - 23 Faraji M, Bazrafshan E, Almasian M, Khoshnamvand N. Investigation of fluoride adsorption from aqueous solutions by modified eucalyptus leaves: isotherm and kinetic and thermodynamic studies. *Iranian Journal of Health Sciences* 2017;5(3):65-77.
 - 24 Ahmadi S, Kord Mostafapour F. Survey of efficiency of dissolved air flotation in removal penicillin G potassium from aqueous solutions. *Brit J Pharma Res* 2017;15(3):1-11.
 - 25 Khoshnamvand N, Ahmadi S, Kord Mostafapour F. Kinetic and isotherm studies on ciprofloxacin an adsorption using magnesium oxide nanoparticles. *J Applied Pharm Sci* 2017;7:079-83.
 - 26 Igwegbe CA, Onyechi PC, Onukwuli OD, Nwokedi IC. Adsorptive treatment of textile wastewater using activated carbon produced from *Mucuna pruriens* seed shells. *World Journal of Engineering and Technology* 2016;4:21-37.
 - 27 Coates J. Interpretation of infrared spectra. A practical approach. In: R.A. Meyers RA. editor. *Encyclopedia of analytical chemistry: applications, theory and instrumentation*. Chichester: John Wiley & Sons Ltd; 2010. pp. 10815–37.
 - 28 Igwegbe CA, Onukwuli OD, Nwabanne JT. Adsorptive removal of Vat Yellow 4 on activated *Mucuna pruriens* (velvet bean) seed shells carbon. *Asian Journal of Chemical Sciences* 2016;1(1):1-16.
 - 29 Samadi MT, Norozi R, Azizian S. Survey impact of activated alumina in fluoride concentration present in water and appointment adsorption isotherm and kinetics. *J Environ Health* 2009;2(3):224-31.
 - 30 Nigussie W, Zewge F, Chandravanshi BS. Removal of excess fluoride from water using waste residue from alum manufacturing process. *J Hazard Mater* 2007;147(3):954-63.
 - 31 Li YH, Wang S, Zhang X, Wei J, UC X, Luan Z, et al. Adsorption of fluoride from water by aligned carbon nanotubes. *Mater Res Bull* 2003;38(3):469-760.
 - 32 Rasheed MA, Jamhour Q. New inorganic ion-exchange material for selective removal of fluoride from potable water using ion-selective electrode. *Am Environ J Sci* 2005;1(1):1-4.
 - 33 Ahmadi S, Rahdar A, Rahdar S, Igwegbe CA, Removal of Remazol Black B from aqueous solution using P- γ -Fe₂O₃ nanoparticles: synthesis, physical characterization, isotherm, kinetic and thermodynamic studies, *Desal Water Treat* 2019;152:401-10.
 - 34 Balarak D, Kord Mostafapour F, Bazrafshan E, Mahvi AH. The equilibrium, kinetic, and thermodynamic parameters of the adsorption of the fluoride ion on to synthetic nano sodalite zeolite. *Fluoride* 2017;50(2):223-34.
 - 35 Zazouli MA, Mahvi AH, Dobaradaran S, Barafrashtehpour M, Mahdavi Y, Balarak D. Adsorption of fluoride from aqueous solution by modified *Azolla filiculoides*. *Fluoride* 2014;47(4):349-58.
 - 36 Ahmadi S, Kord Mostafapour F. Adsorptive removal of aniline from aqueous solutions by *Pistacia atlantica* (Baneh) shells: isotherm and kinetic studies. *J Sci Technol Environ Inform* 2017;5(01):327-35.
 - 37 Salaryan P, Mokari F, Saleh Mohammadnia M, Khalilpour M. The survey of linear and non-linear methods of pseudo-second order kinetic in adsorption of Co(II) from aqueous solutions. *Int J Water Wastewater Treat* 2013;1:130-4.